Single Pulse Neutron and Gamma Discrimination with Combination Glass and Liquid Hybrid Detector

Gregory Hill

A senior thesis submitted to the faculty of
Brigham Young University
in partial fulfillment of the requirements for the degree of

Bachelor of Science

Lawrence Rees, Advisor

Department of Physics and Astronomy

Brigham Young University

April 2016

ABSTRACT

Single Pulse Neutron and Gamma Discrimination with
Combination Glass and Liquid Hybrid Detector

Gregory Hill
Department of Physics and Astronomy, BYU
Bachelor of Science

The discrimination of neutrons and gamma rays has become an important field of research both for scientific purposes as well as security purposes. Until recently helium-3 was used to discriminate neutron radiation from gamma radiation, however, with the depletion of helium-3 reserves, new methods must be found. The BYU Nuclear Research Group has developed a hybrid lithium-6 glass and liquid scintillator that combines the discrimination characteristics of both materials. Parameters such as pulse area, area distribution, and after peaking count are used to sort the gammas and neutrons into different regions. Particularly, the single pulse analysis methods as well as data analysis improvements are reported. These improvements provide tools for double pulse analysis. Future detector innovations are also discussed.

Keywords: Gamma, Neutron, Radiation Discrimination, Lithium Glass, Pulse Shape Discrimination

ACKNOWLEDGMENTS

Thanks to Andrew McClellan and John Ellswort, Financial Suppport From the National Nuclear Security Administration Grant #DE-FG52-10NA29655 and Department of Homeland Security Grant #2010-DN-077-ARI039-02, prose was streamlined to prevent confusion. Charts were refined and better placed

Contents

Table of Contents **iv**

List of Figures **1**

1 Introduction **2**
1.1 Purpose 2
1.2 Background 2
1.3 Project Overview 4

2 Experimental Setup **5**
2.1 Physical Setup 5
2.2 Electronic setup 7
2.3 Signal Analysis 9

3 Results **14**
3.1 Comparative Performace 14
3.2 The Californium Results 18
3.3 The Cobalt Results 18
3.4 Discrimination Error 18
3.5 The future 19

Bibliography **21**

Index **22**

List of Figures

2.1 Physical Layout of Dector 6

2.2 Detector Schematic 8

2.3 Typical Glass Neutron Event 10

2.4 Typical Liguid Gamma Event 10

2.5 Typical Glass Gamma Event 11

2.6 Typical Liquid Neutron Event 11

2.7 The chart displays the user defined parameters as seen in anspec. A) is called the Early Line this defines the start of area integration, B) is the Early/Late line. The area to the left the early area and the right is the late area, this is used to asses the distribution of the area within the pulse, C) is the late line. This defines the end of the pulse, D) is the After-Peaking threshold. Peaks above this value are added to the after peaking count for this pulse. 13

3.1 Fraction Early vs Area: Californium 15

3.2 Fraction Early vs Area: Cobalt 16

3.3 Fraction Early vs Area: Background 17

Chapter 1

Introduction

1.1 Purpose

Since the discovery of radioactive decay, radiation detection and discrimination have been vital tools of science. These tools uses include both probing into the composition of matter and environmental safety. Distinguishing between neutron radiation and gamma radiation is of particular importance due to the hazardous nature of the substances that emit these forms of radiation. In this thesis, new techniques of detector construction to better distinguish between gammas and neutrons is explored, explicitly the combination of a lithium-6 detector and a liquid scintillator is used to produce distinct light outputs analyzed using new single pulse discrimination techniques.

1.2 Background

Neutron radiation is typically indicative of very heavy elements and is associated with nuclear fission. One factor that makes detecting neutrons difficult is the neutron's lack of charge causes it to have limited interaction with surrounding material in a measurable way. Thus the techniques used to detect charge-bearing radiation cannot be used to detect neutrons. Unfortunately, the materials

that interact with neutrons in a discernable way are also sensative to gamma radiation, making discrimination of the two types of radiation difficult.

Up until 2010, the most commonly used material for neutron detection was helium-3(^{3}He). This isotope of helium has a very large neutron cross section of about 5330 barns [1]. This means that it has a high capacity to interact with neutrons through neutron capture. Additionally the ^{3}He interacts very little with gamma radiation unlike most other scintillation materials. Additionally, helium is non toxic, inert and easy to use, making it an ideal research tool. However, with the events of September 11th, ^{3}He based detectors were widely deployed to safeguard against radiological material from entering the country and the previously plentiful supplies of ^{3}He were depleted. Presently cost of ^{3}He runs at $2000 a liter making it extremely difficult to obtain in useful quantities [2]. Due to this shortage, alternatives are being researched. Alternatives do exist but none with ease of use and discrimination capabilities of ^{3}He.

Some of these alternatives include organic scintillators, lithium-6 glass and cadmium based detectors [3], all utilize typically two mechanisms; proton recoil pulse, and neutron capture. Proton recoil is caused when the neutron directly strikes a very light nucleus and imparts some or all of its momentum to it. The kinetic energy of the nucleus is passed from the medium to a scintillator material that emits light. Neutron capture occurs when the neutron encounters a nucleus that is readily able to absorb it. When this occurs, the nucleus is left in an excited state. It can lose this excess energy by processes including gamma emission, particle emission, and fission [1].

The photons produced by the scintillator enters a photomultiplier tube (PMT) which utilizes the photoelectric effect through multiple stages to create a measurable current. This current is fed through amplifiers and then into an analog-to-digital converter (ADC) or signal digitizer and then recorded by a computer for analysis.

1.3 Project Overview

The materials used in the BYU Nuclear Physics Group's detector are Ej 325, a liquid mineral oil based scintillator, and lithium-6 glass. The Ej 325 utilizes proton recoil to diminish the neutrons energy and produce a signal pulse. The lithium-6 glass captures the slowed neutrons and then fissions into an alpha and a triton [1]. Unfortunately these materials, while fairly economical, also react readily to gamma radiation as well. The main form of gamma interaction is Compton scattering, which releases an electron that can cause responses similar to the proton recoil pulse and is mistakable for a neutron especially at lower energies. It is hoped, however, that the combination of the two scintillators can be used to compensate for their individual weaknesses.

Chapter 2

Experimental Setup

2.1 Physical Setup

As described previously, this detector utilizes two different detector types simultaneously, however their specific arrangement is also vital to the detector's workings. The entire scintillator unit is contained in a rectangular glass container with a base of internal dimension of 5in by 5in. The lithium glass sheet has a diameter of 5in and is placed at the bottom of the container. Then, 6.5cm of Ej 325 liquid scintillator is poured on top of this.

The Ej 325 was selected against other formulations of scintillator for several reasons. It provides reasonably different light response to gamma and neutron interactions as well as being fairly chemically stable [4]. There are liquids better at discrimination than the EJ 325, but usually at the expense of being highly volatile. This would require a much more involved setup to safely contain the fluid.

The stability of liquid scintillator is important due to the need to bubble the fluid with argon to provide peak discrimination performance [5]. In addition to the setup already described, a tube bringing argon gas into the container is also inserted beside the PMT. Oxygen dissolved into the

fluid suppresses the light output of the scintillator. To fix this the oxygen is flushed out by piping either nitrogen or argon through the fluid. This must be done periodically to maintain the proper performance of the scintillator.

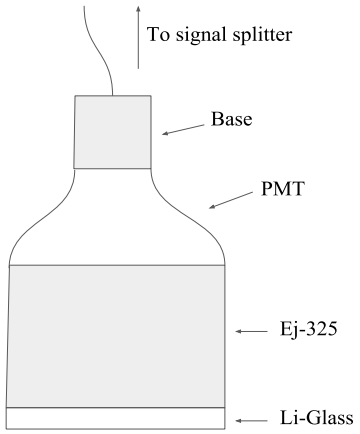

Figure 2.1 The PMT sits above 5cm of Ej 325 scintillating fluid that both detects the radiation and moderates it for better interaction with the 1mm thick lithium-6 glass plate.

The depth of 6.5cm was experimentally determined to provide the best performance for the lithium glass. The lithium glass' primary method of neutron interaction is through neutron capture, however, to capture the neutrons successfully, the incoming neutrons need to be at a sufficiently low energy. In addition to scintillating in response to the proton recoil, the liquid scintillator also moderates the neutron's energy. With enough moderation, the incoming neutrons will settle into a neutron "cloud" [1]. If the lithium glass is placed within the neutron cloud, it will be most able to capture the neutrons, improving its efficiency. This is the reason for the particular depth of the fluid and the placement of the glass within it. The face of the PMT is then set just barely into the liquid. The Adit PMT is powered by a 1200V power supply. The entire detector assembly is contained in a light tight wooden box to prevent damage to the PMT. The different radioactive sources are placed beneath the box at different distances so the activity rate seen by the detector is the same for each source.

2.2 Electronic setup

One of the difficulties of this setup is that the glass and the liquid have very different light intensity responses. The liquid's response is much brighter than that of the lithium glass. Typically a single PMT's output is fed to a single amplifier and then into a digitizer. However, the best amplification for seeing the glass output is so high that the liquid output is clipped. Conversely, the amplification settings best for the liquid are too low to pick out the weaker glass signal. Finally, the digitizer has very limited voltage range it can handle before sustaining damage. These factors combine to make using a single PMT detector difficult.

The solution to this problem was to split the signal and process the two streams differently before recombining them. Specifically, the signal is split at a 50 ohm splitter after leaving the PMT. The 50 ohm spliter prevents ringing in the system. After the 50 ohm tee the signals are passed through identical length cables to two separate amplifiers. One of the amplifiers is set to a very high amplification so as to best view the glass events, while the other is set fairly low so to view the liquid events best. From the amplifiers the signal goes through a 10dB attenuator on the lower voltage signal and a 20dB attenuator for the higher voltage amplifier to protect the digitizer and into two separate channels on the digitizer.

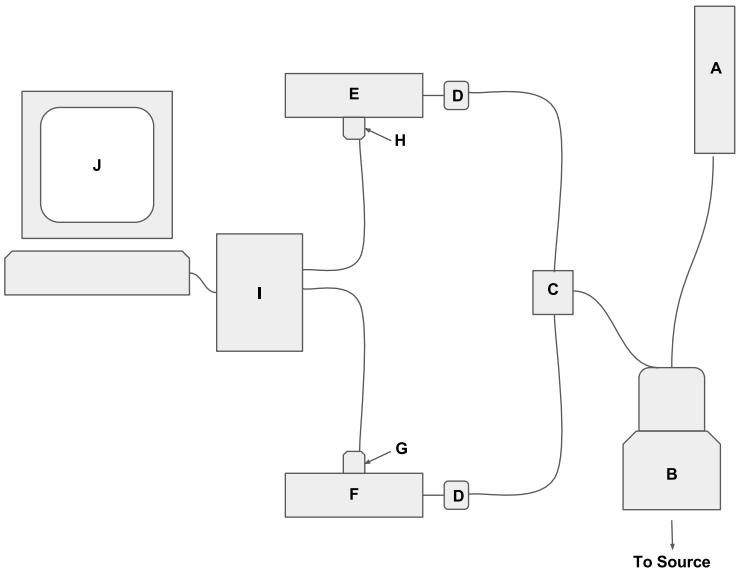

Figure 2.2 A schematic of the detector setup, the constituants are as follows. A) Ortec power supply set for 1200 volts, B) Adit Photomultiplier tube and base, C) 50Ω T splitter, D) 100Ω terminators, E) Amplifer set for low amplification, F) Amplifier set for high amplification, G) 20dB Attenuator, H) 10dB Attenuator, I) CEAN digitizer with the inputs in two different channels, J) Analysis Terminal

The signal is captured by a BYU produced digitizer controller as two separate files. The program is set to capture both channels simultaneously when one is triggered. The channel receiving the strong signal is set to be the trigger channel since any response from either source will be large enough to trigger the capture. The minimum trigger threshold is set to 100mV. This value was experimentally determined to provide the best distinction between signal and noise. When the system is triggered both channels are recorded at the same time giving a version of the signal with both high and low amplification.

For single pulse discrimination each signal trigger causes the digitizer to record the voltage level for 512 time intervals of 4ns each. These intervals are commonly referred to as channels. When the device first triggers, it records the 80 channels preceding the trigger and then a further 432 channels afterword. This means rather than recording the event pulse only partway through,

the event is cleanly recorded with some leeway before and after the event.

With the two channels recorded separately they can be analyzed and recombined as a single signal using Matlab code written by the BYU Nuclear Physics Group. This is done by utilizing the fact that the one channel has the correct shape for all the pulses but is very small and the other has the preferred size but some of its larger pulses get clipped. There are events that look acceptable in both channels and can be used to determine an amplification ratio between the two channels. These events are selected by determining whether the larger version has been clipped, this has been experimentally determined for this amplifier to be when its output goes above 6.4V. If the event is below this threshold, its maximum peak height is compared against its smaller version and the maximum height of the larger signal is divided by the smaller peak height to gain an amplification ratio. This test is run for each event pair in the data set and an overall amplification ratio is found by averaging each pair's ratio. This ratio is then used to amplify the smaller signal to the level of the larger, except without the clipping and the limits on the max voltage imposed by the digitizer. This yields a single signal with the correct pulse shape and relative pulse height that can display both weak signals and very large signals successfully.

The file containing voltage values for each event is read into a Matlab analysis suite called Anspec developed by our research group. Each pulse is read in and analyzed for certain traits that can be used to tell different kinds of pulses apart. Although there are many different traits that can be considered, the ones found best able to discriminate pulse types will be discussed.

2.3 Signal Analysis

Before describing the the analysis techniques used, it is useful to look at what some of the typical pulse shapes are. Following are examples of the different scintilltion materials interacting with the different types of radiation in question as well as descriptions on the traits that distinguishes them.

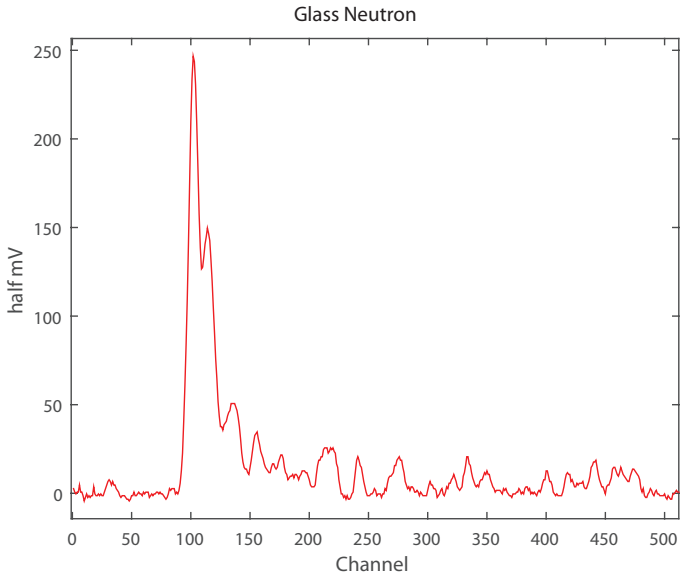

Figure 2.3 This is a typical lithium glass pulse from a neutron interaction. Note the comparetively short pulse height and the numerous after-peaks

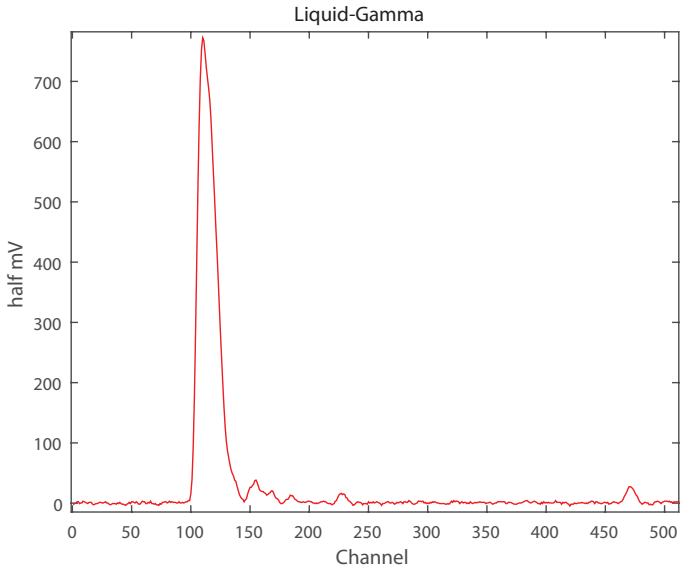

Figure 2.4 This is a typical interaction of the gamma radiation and the liquid scintillator. These peaks are the sharpest and usually the tallest.

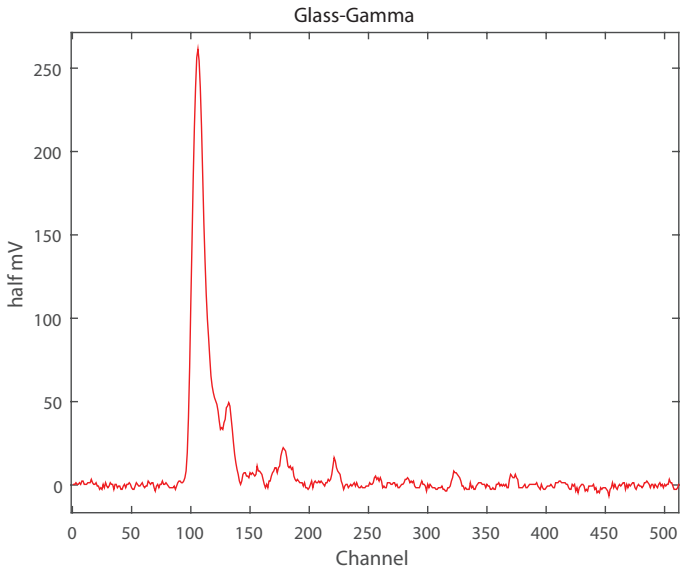

Figure 2.5 Typical glass pulse from a gamma interaction, also note the shorter peak height but smaller number of after-peaks.

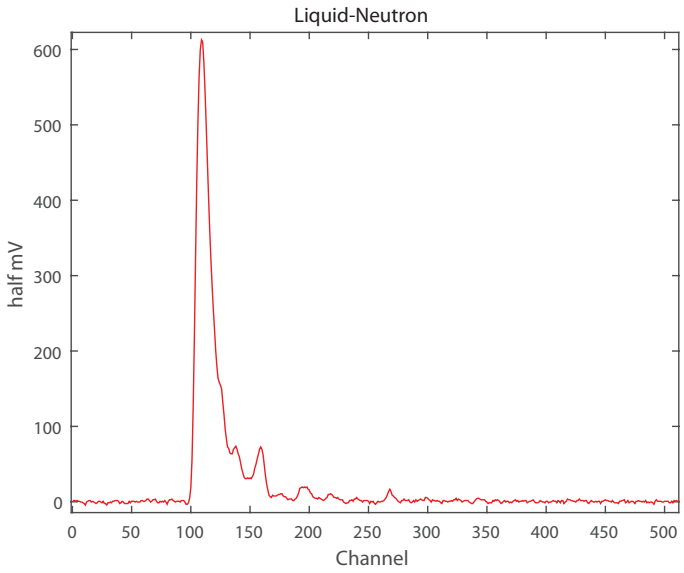

Figure 2.6 Typical liquid scintillator and neutron interaction, notice the larger longer tailing region the peak has.

Area under the curve provides one of the best sources of discrimination even when the neutron energies and gamma energies are similar. This is calculated by simply summing the value of

the discrete voltage levels of the pulse recorded in the file captured by the digitizer, similar to a Riemann sum. This value provides reliable discrimination even if the pulse height is similar as gamma pulses tend to be sharper peaks and the neutron pulses tend to have longer tails giving them a different area.

Another useful characteristic is referred to as "fraction early". This is essentially a measure of how much of the pulse's area comes by a fixed time after the start of the pulse. What point of the pulse is considered to be fraction early is determined by the user. The criteria for choosing the point is discussed in a later section. In this program the fraction early is a value from 0 to 1, 0 meaning that none of the area falls within the area designated as the early part of the pulse and 1 meaning that all of the area falls within in the early section. This is calculated by simply doing the same summation as the area except it only goes until the time point specified by the user. This sum is then divided by the sum of the entire area. This trait draws upon the difference in shape between gamma and neutron pulses, the gamma pulses usually having a larger fraction early.

The last trait is referred to as "after-pulsing count". This trait is a measure of how many small after-peaks follow the primary peak. This is calculated by counting the number of peaks above a certain threshold set by the user. If the threshold is set too low, the computer will be counting noise, but if it is too high it will not be able to discriminate well. This trait utilizes the fact that when the neutron strikes the liquid it recoils off a series of protons and causes smaller subsequent peaks. Thus, neutron events tend to have a larger number of after-peaks.

The aforementioned characteristics are measured using several user defined parameters. The early line is specified as being a user-selected number of channels before the main peak. This defines the start of the pulse area. The corresponding late line is a user-defined number of channels after the the main peak that defines the end of the pulse The early/late line is a line placed in a user-defined position between the other two lines and defines what portion is regarded as the early area and the late area. The placement of these lines is chosen by the user after viewing a suitable

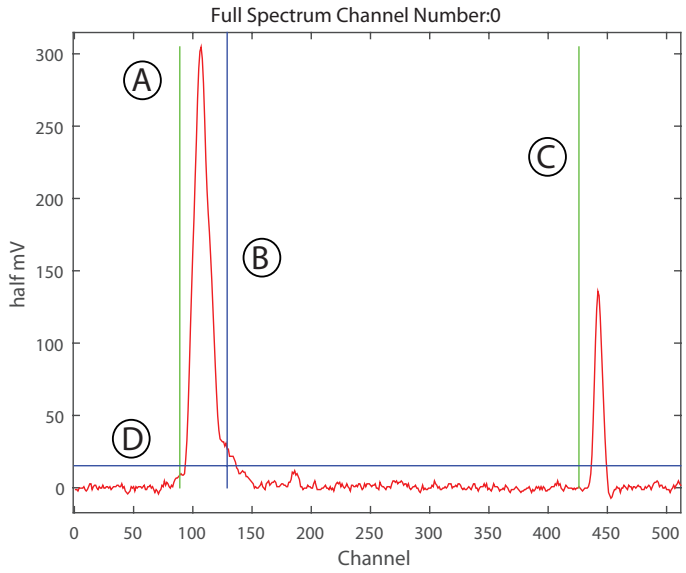

Figure 2.7 The chart displays the user defined parameters as seen in anspec. A) is called the Early Line this defines the start of area integration, B) is the Early/Late line. The area to the left the early area and the right is the late area, this is used to asses the distribution of the area within the pulse, C) is the late line. This defines the end of the pulse, D) is the After-Peaking threshold. Peaks above this value are added to the after peaking count for this pulse.

number of pulses to check that they will provide the desired discrimination and are then applied to the whole data set. The numerical values of the traits mentioned are recorded for each pulse and then graphed on scatter plots. The separation of the regions will be reviewed in the results section.

Chapter 3

Results

3.1 Comparative Performace

This particular detector setup yields a unique distribution for both the neutron source and the gamma source. As mentioned in the previous sections, the most discriminating plot was the Fraction Early vs. Area. In addition to this parameter we also incorporated the after peaking count into our discrimination. Below follows a series of fraction early vs. area plots for the same source for different after-peaking counts. The charts proceed left to right, top to bottom by showing only the data points with zero after-peaks and then 1,2,3 peaks etc. The last chart shows all the points with 11 after-peaks or more.The after peaking count is simply a measure of how many peaks after the tallest main peak are above a certain user defined threshold.

Figure 3.1 Fraction Early vs Area: Californium

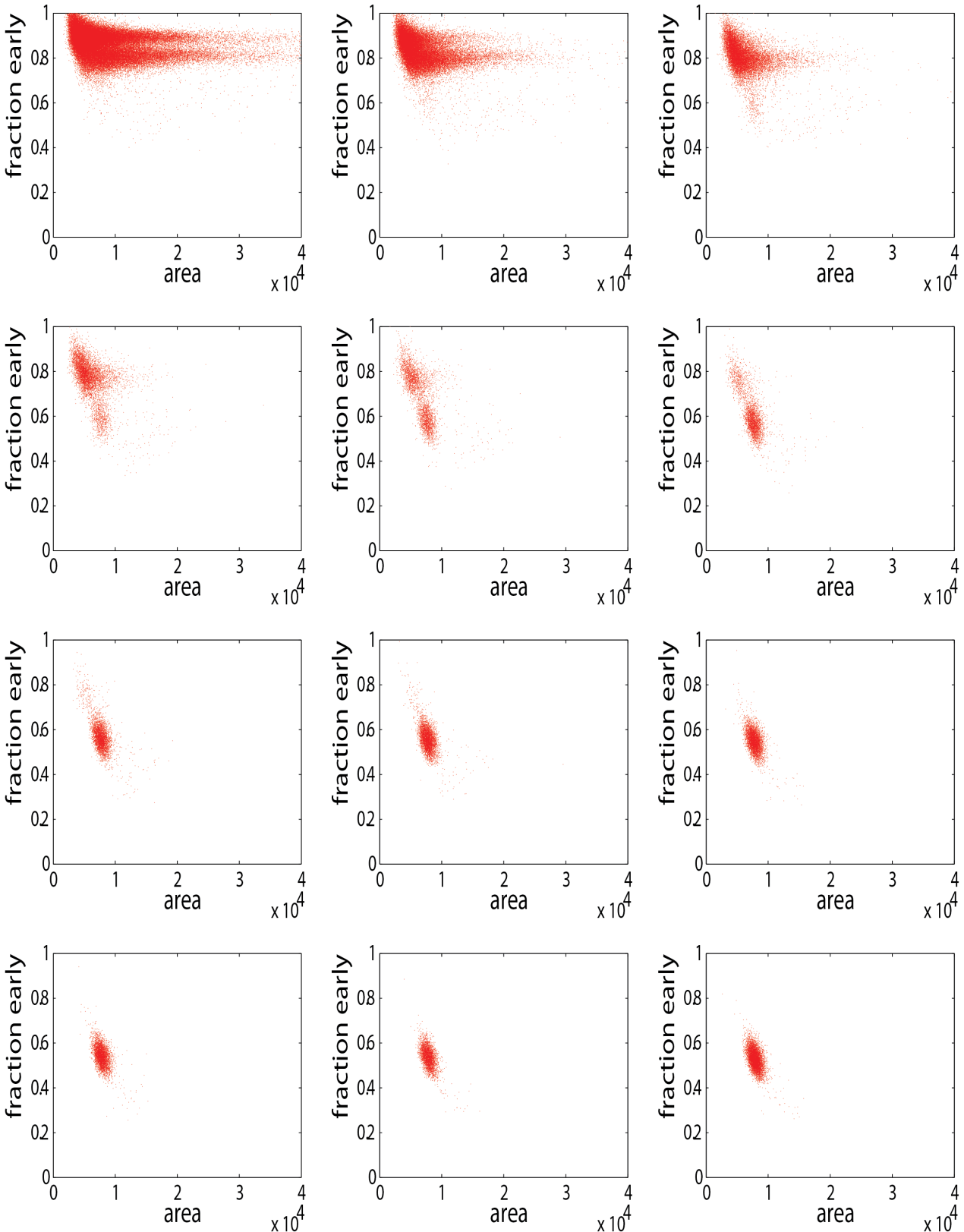

Figure 3.2 Fraction Early vs Area: Cobalt

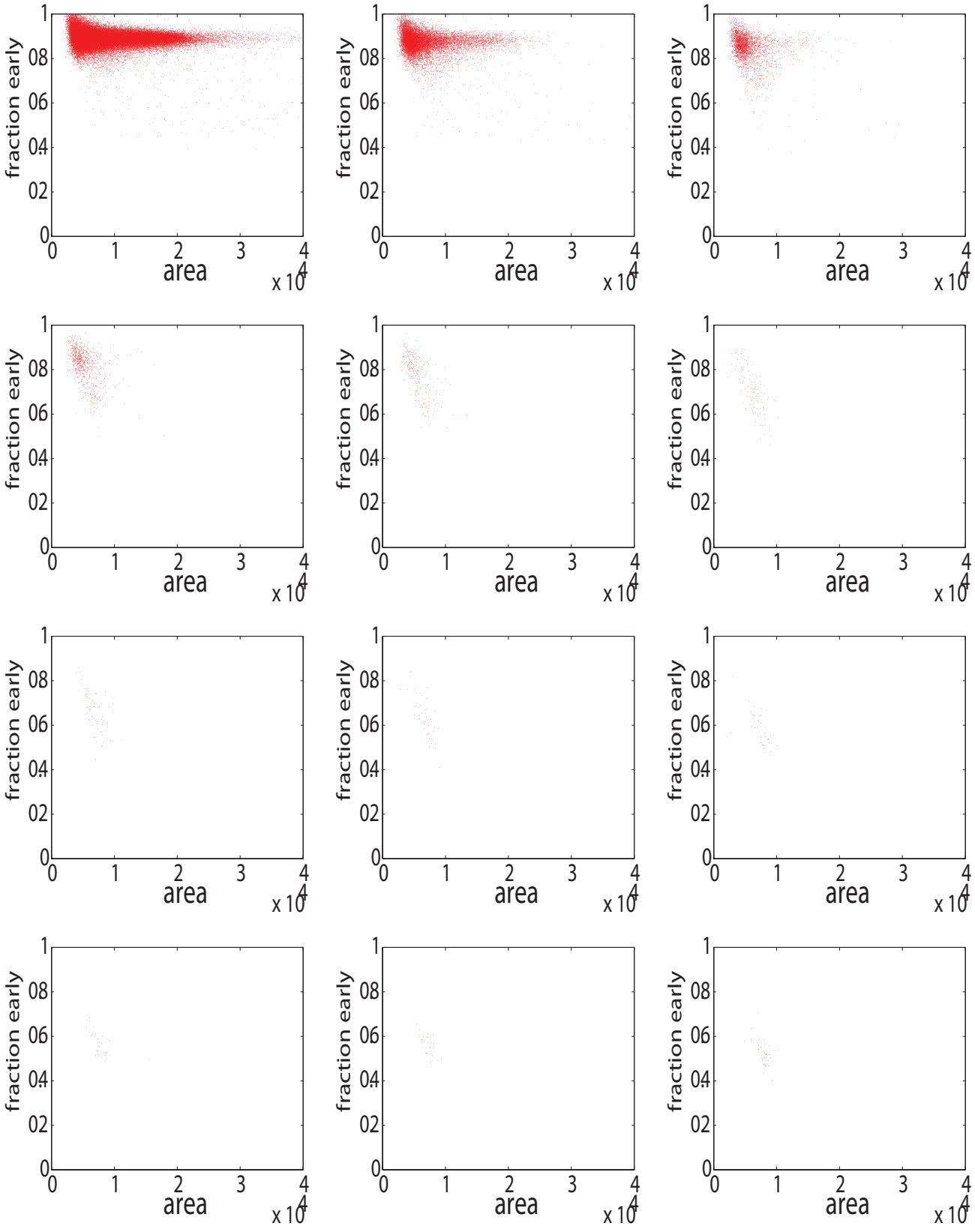

Figure 3.3 Fraction Early vs Area: Background

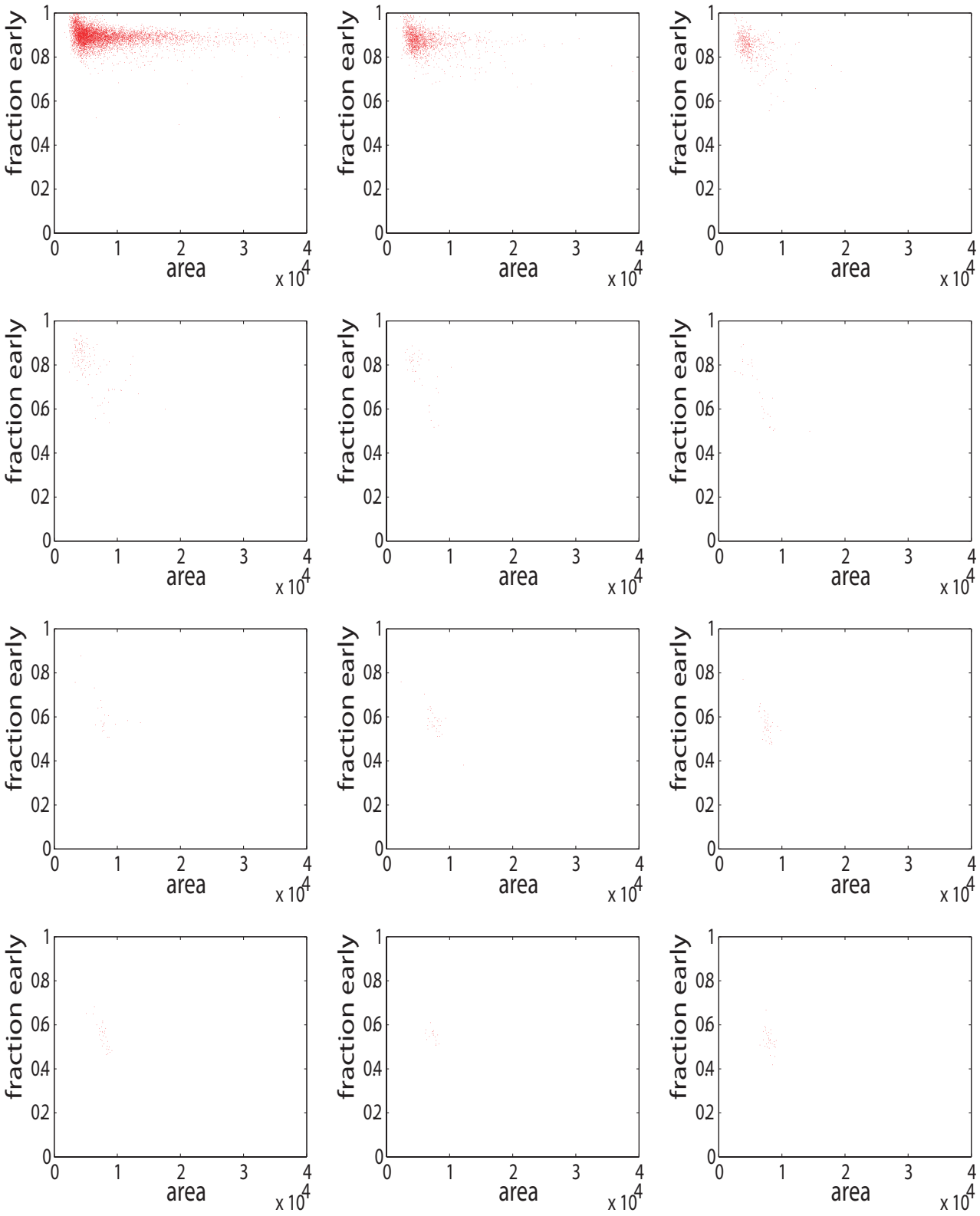

3.2 The Californium Results

We can see that within a count of two after-peaks the results that we have identified as being part of the liquid response have been accounted for, and for a count of 3 peaks and on we are left with what is typically identified as being glass events. We also see that the region corresponding to neutron capture has an extremely high after-peak count compared to the regions associated with gamma events, proving it to be an excellent discrimination characteristic.

3.3 The Cobalt Results

Since cobalt emits only gamma radiation, the cobalt charts distinctly show the difference in the regions that can be associated with gammas and neutrons. By also comparing it to the background radiation charts it shows that most, if not all the, events in the cobalt charts that are still in the neutron region of the high after-peaking graphs are background events.

3.4 Discrimination Error

The original goal of this research was to develop a detector that can discriminate gamma radiation from neutron radiation especially for the purpose of neutron source detection. The discrimination error is determined using industry standard techniques. Using the known activity rates of the sources, known ratios of radiation types per decay event, and the solid angle for the detector setup, the amount of gamma and neutron radiation incident on the detector material is calculated. Then regions of interest are selected from the fraction early vs. area chart of interest and the background counts in that region are subtracted out. The remaining number of counts in the region is divided by the total number of counts incident on the detector. Thus, to calculate the error, the number of gamma events from a cobalt source that end up in the region associated with neutrons is divided

by the number of gamma events that are calculated to be incident on the detector during the data acquisition. The efficiency is calculated the same way except a neutron source is used and the number of neutrons incident on the detector is used.

At zero after-peaking the detector runs at an efficiency of 15%. Meaning that just 15% of the total number of neutrons incident on the detector are detected in the region of interest. This may seem low, however, just because the neutron was incident on the detector face does not mean that they interact with the scintillation material. Also at zero after-peaking there is a misidentification error of 3.6×10^{-5}. As the after-peaking is increased the efficiency drops incrementally, but the misidentification ratio improves. At an after-peaking count of 10 and and greater the efficiency has dropped to 6.5% but the misidentification ratio improves to 5.17×10^{-6}. The Homeland Security desired discrimination ratio is 1×10^{-6}. This that present detector while less efficient than others has a precision near to that of helium-3.

3.5 The future

These advances in single pulse analysis provide a strong basis for what is referred to as double pulse analysis. In double-pulse analysis, a neutron must first recoil off the liquid scintillator to lose kinetic energy and then is ultimately captured by the lithium-6. So, in addition to the shape of the pulses, the timing and order is also a factor in discrimination. This method, while less efficient, has very little discrimination error. The better we are able to determine what each individual peak is, the more easily we are able to determine when the double pulses meet the desired criteria.

Another expected avenue of research uses broken lithium glass fragments rather than solid sheets. As is stated earlier in the paper, the main mechanism by which the lithium-6 glass interacts with gammas is through Compton scattering. The released electrons propagate through the glass causing pulses that seem similar to those caused by the alpha triton pair which may confuse dis-

crimination. However, if the glass is broken, the alpha triton pair with their very short mean free path with deposit all off their energy within the glass shard, but the electrons will exit the glass relatively quickly and deposit little of their energy. This should substantially change the appearance the gamma pulses.

This should enable us to produce a detector that has comparable performance to helium-3 without the the extreme cost of helium-3. This will enable smaller research institutions to conduct radiation research with less cost.

Bibliography

[1] G. F. Knoll, *Radiation detection and measurement* (John Wiley & Sons, 2010).

[2] D. A. Shea and D. Morgan, "The Helium-3 Shortage: Supply, Demand, and Options for Congress," (2015).

[3] T. Jex, "Preliminary Study of a Dual PMT Lithium-Cadmium Hybrid Neutron Detector,", Senior Thesis, 2014, brigham Young University, Provo, UT.

[4] E. Technology, "EJ-325A MINERAL OIL BASED LIQUID SCINTILLATOR WITH PSD PROPERTY,", 2013.

[5] X. Hua-Lin, "Oxygen quenching in LAB based liquid scintillator and nitrogen bubbling," Chin. Phys. **C34,** 571–575 (2010).

Index

After Pulsing, 12
Amplifiers, 7
Area, 11
Argon Bubbling, 5

Californium, 18
Cobalt, 18

Efficiency, 19
Ej 325, 4, 5, 10, 11
Error, 19
expand ADC range, 9

Fraction Early, 12

Helium 3, 3

Lithium - 6 Glass, 4, 5, 10, 11

neutron capture, 3
Neutron Cloud, 6

PMT, 3, 6
proton recoil pulse, 3
Pulse Shape, 9

Signal Clipping, 9

Threshold, 8
Time Channels, 8

User Defined Parameters, 12